ISSN 1330–0008
CODEN FIZAE4

INFLUENCE OF CROSSED ELECTRIC AND QUANTIZING MAGNETIC FIELDS ON THE EFFECTIVE ELECTRON MASS IN SEMICONDUCTOR SUPERLATTICES

KAMAKHYA P. GHATAK and SHAMBHU N. BANIK*

Department of Electronic Science, University of Calcutta, University College of Science and Technology, 92, Acharya Prafulla Chandra Road, Calcutta 700009, India
**Department of Physics, Dandirhat Nagendra Kumar Uchcha Siksha Niketan, P. O. Dandirhat, Dt. North 24 Parganas, West Bengal, India*

Received 9 August 1994

Revised manuscript received 24 March 1995

UDC 538.915

PACS 71.25.Jd

An attempt is made to study the effective electron mass at the Fermi level in semiconductor superlattices under cross–field configuration and to compare it with that of the constituent materials, taking GaAs/AlAs superlattice as an example. It is found that the effective electron masses along both directions depend also on the magnetic quantum number. The characteristic feature of the cross–field is to introduce index–dependent oscillatory mass anisotropy in the constituent materials. The numerical values of the mass in superlattices are greater than of the forming compounds. The corresponding well–known results in the absence of electric field have also been obtained from our generalized analysis under certain limiting conditions.

1. Introduction

The effective mass of the carriers in semiconducting materials, which is strongly connected with the carrier mobility, is known to be one of the most important parameters of semiconductor devices [1]. In materials with parabolic dispersion relation, the effective mass is independent of energy, whereas for non–parabolic specimens the same mass varies significantly with carrier energy. It must be mentioned that among the various definitions of the effective electron mass [2], it is the momentum effective mass that should be regarded as the basic quantity [3]. This is due to the fact that it is the momentum effective mass that apears in the description of the transport phenomena and all other properties of the electron gas in a band with arbitrary band non–parabolicity [3]. It can be shown that it is this effective mass which enters in various transport coefficients and plays the most dominant role in explaining the experimental results of different types of scattering mechanisms [4]. The carrier degeneracy in semiconducting materials influences the effective mass when it is energy dependent. Under degenerate conditions and at low temperatures, where the quantum effects become prominent, only the electrons at the Fermi surface of n-type materials participate in the conducting process. Hence, the effective momentum mass of the electrons (hereafter referred to as EMM) corresponding to the Fermi energy would be of interest in electron transport under such conditions. The Fermi energy is again determined by the electron energy spectrum and the electron statistics and, therefore, these two features would determine the dependence of the EMM on the degree of degeneracy.

In recent years, various dispersion relations for different specimens have been proposed, which have created the interest for studying the EMM in such electronic materials under various physical conditions [5-10]. Besides, with the advent of molecular beam epitaxy, fine line lithography, organometallic chemical vapour phase deposition and other experimental techniques, it has become possible to grow semiconductor superlattices (SL's), the new type of electronic materials. The SL has found wide applications in many new device structures, such as photodiodes [11], photodetectors [12], transistors [13], light emitters [14], electro–optic modulators [15] and other devices. Though extensive work has already been done on the various electronic properties of such heterostructures, nevertheless it appears from the literature that the EMM under cross–field configuration in SL's has yet to be studied. In this connection we wish to note that the investigations of the electrons in electronic materials in the presence of the crossed electric and magnetic fields offer interesting physical possibilities, both experimental and theoretical [16]. The cross–field configuration is fundamental for studying the classical and quantum transport in solids [17]. In this paper, we investigate the doping and magnetic field dependences of the EMM in SL and that of the corresponding bulk materials in the presence of crossed electric and quantizing magnetic fields, taking GaAs/AlAs SL as an example.

2. *Theoretical background*

In the presence of a quantizing magnetic field B along the SL direction and the crossed electric field E_0 along the x-axis, the Hamiltonian H takes the form

$$H = \frac{\hat{p}_x^2}{2m^*} + \frac{(\hat{p}_y - eB\hat{x})^2}{2m^*} + E_{0s} - E_{1s}\cos\left(\frac{2\pi\hat{p}_z}{\hbar k_0}\right) - eE_0\hat{x} \tag{1}$$

where the hats denote the respective operators and the other symbols are defined in Ref. 18. The modified electron energy spectrum for SL's, including spins, reads

$$\epsilon = \left(n+\frac{1}{2}\right)\hbar\omega_0 - \frac{eE_0 p_y}{m^*\omega_0} \pm \frac{1}{2}g_0\mu_0 B -$$

$$-\frac{e^2E_0^2}{2m^*\omega_0^2} + E_{0s} - E_{1s}\cos\left(\frac{2\pi k_z}{k_0}\right) \tag{2}$$

where ϵ is the electron energy in the presence of crossed electric and magnetic fields as measured from the edge of the material with smaller band gap in the absence of crossed–field configuration, $n = 0, 1, 2, ...$ is the Landau quantum number, $\omega_0 = eB/m^*$ is the cyclotron frequency, g_0 is the band edge g factor and μ_0 is the Bohr magneton. In non–parabolic energy bands, the EMM along any direction has to be obtained by dividing the momentum along this direction by the velocity along this specified direction [8]. Thus the use of Eq. (2) leads to the expressions of EMM's along z and y directions, respectively, as

$$m_z^*(n, E_F) = \hbar^2 k_z \frac{\partial k_z}{\partial E}\Big|_{p_y=0, E=E_F} = \frac{\hbar^2}{E_{1s}d_0^2}\frac{1}{\sqrt{1-[D_\pm(n,E_F)]^2}}\cos^{-1}[D_\pm(n,E_F)] \tag{3}$$

and

$$m_y^*(n, E_F) = \hbar^2 k_y \frac{\partial k_y}{\partial E}\Big|_{k_z=0, E=E_F}\left(\frac{m^*\omega_0}{eE_0}\right)^2 \times$$

$$\times\left[E_F - \left(n+\frac{1}{2}\right)\hbar\omega_0 + E_{1s} - E_{0s} \pm \frac{g_0\mu_0 B}{2} + \frac{e^2E_0^2}{2m^*\omega_0^2}\right] \tag{4}$$

where d_0 is the SL period,

$$D_\pm(n, E_F) = \frac{1}{E_{1s}}\left[\left(n+\frac{1}{2}\right)\hbar\omega_0 \pm \frac{g_0\mu_0 B}{2} - \frac{e^2E_0^2}{2m^*\omega_0^2} + E_{0s} - E_F\right]$$

and E_F is the Fermi energy in the present case. It appears from Eqs. (3) and (4) that the evaluations of $m_z^*(n, E_F)$ and $m_z^*(n, E_F)$ as functions of doping require an expression for electron concentration. Considering only the lowest miniband, since for an actual SL only the lowermost miniband is significantly populated at low temperatures where the quantum effects become prominent, the electron statistics can be expressed extending results of Ref. 19 to the present case, including both spin and broadening effects, as

$$n_0 = \frac{-1}{2d_0\pi^2}\sum_{n=0}^{n_{max}}\left[\text{Real part of}\int_{A_0}^{\infty}\left(\int_{x_2}^{x_1} k_z(E^{'})\mathrm{d}k_y\right)\left(\frac{\partial f_0(\epsilon)}{\partial\epsilon}\right)\mathrm{d}\epsilon\right] \tag{5a}$$

where

$$A_0 = \left(n+\frac{1}{2}\right)\hbar\omega_0 - \pm\frac{1}{2}g_0\mu_0 B - \frac{e^2E_0^2}{2m^*\omega_0^2} + E_{0s} - E_{1s},$$

$E^{'} = E_F + \mathrm{i}\Gamma$, $\mathrm{i} = \sqrt{-1}$, $\Gamma = \pi k_B T_D$, k_B is the Boltzmann constant, T_D is the Dingle temperature, $x_2 = -m^*E_0/2B\hbar$, $x_1 = eBd_0\hbar^{-1} + x_2$ and $f_0(\epsilon)$ is the Fermi–Dirac occupation probability factor.

The generalized Sommerfeld's lemma can be written as [20]

$$\int_A^{\infty}\phi(\epsilon)\frac{\partial f_0(\epsilon)}{\partial\epsilon}\mathrm{d}\epsilon = \phi(E_F) + \sum_{r=1}^{t}\nabla_r[\phi(E_F)], \tag{5b}$$

where r is the set of real positive integer whose upper limit is t,

$$\nabla_r = 2(k_BT)^{2r}(1-2^{1-2r})\zeta(2r)\frac{\mathrm{d}^{2r}}{\mathrm{d}E_F^{2r}},$$

T is the temperature, $\zeta(2r)$ is the zeta function of order $(2r)$ and A is the constant.

Thus using Eqs. (2), (5a) and (5b) we get

$$n_0 = C_0\sum_{n=0}^{n_{max}}[P(E_F) + Q(E_F)] \tag{5c}$$

where

$$C_0 = \frac{m^*\omega_0 E_{1s}}{2eE_0\hbar\pi^2 d_0^2},$$

$$P(E_F) = \text{Real part of}\Big[\sqrt{1-(a_1-b_1x_1)^2} - (a_1-b_1x_1)\cos^{-1}(a_1-b_1x_1) -$$

$$-\sqrt{1-(a_1-b_1x_2)^2}+(a_1-b_1x_2)\cos^{-1}(a_1-b_1x_2)\Big],$$

$$a_1=(E_{1s})^{-1}\left[E_{0s}+\left(n+\frac{1}{2}\right)\hbar\omega_0-\frac{e^2E_0^2}{2m^*\omega_0^2}-E_F-\mathrm{i}\Gamma\right],$$

$$Q(E_F)=\sum_{r=1}^{t}\nabla_r[P(E_F)].$$

We shall now derive the expressions for the EMM's and n_0 in the corresponding bulk materials having parabolic energy bands for the purpose of comparison with superlattices under cross–field configuration. The dispersion relation for the bulk material can be written as [17]

$$\epsilon=\left(n+\frac{1}{2}\right)\hbar\omega+\frac{\hbar^2k_z^2}{2m^*}\pm\frac{1}{2}g_0\mu_0B-\frac{eE_0p_y}{m^*\omega_0}-\frac{e^2E_0^2}{2m^*\omega_0^2}. \tag{6}$$

The use of Eq. (6) leads to the expressions of EMM's and n_0, respectively, as

$$m_z^*(n,E_F)=m^*, \tag{7}$$

$$m_y^*(n,E_F)=\left(\frac{m^*\omega_0}{eE_0}\right)^2\left[E_F-\left(n+\frac{1}{2}\right)\hbar\omega_0\pm\frac{1}{2}g_0\mu_0B+\frac{e^2E_0^2}{2m^*\omega_0^2}\right] \tag{8}$$

and

$$n_0=C_1\sum_{n=0}^{n_{max}}[U(E_F)+V(E_F)] \tag{9}$$

where

$$C_1=\frac{\sqrt{2m^*}B}{3E_0\pi^2\hbar^2L_x},$$

$$U(E_F)=\text{Real part of}\left\{\left[E_F+\mathrm{i}\Gamma-\left(n+\frac{1}{2}\right)\hbar\omega_0+eE_0L_x-\frac{m^*E_0^2}{2B^2}\right\}^{3/2}-\right.$$

$$- \left\{ E_F + \mathrm{i}\Gamma - \left(n + \frac{1}{2}\right) \hbar\omega_0 - \frac{m^* E_0^2}{2B^2} \right\}^{3/2} \Bigg]$$

and

$$V(E_F) = \sum_{r=1}^{t} \nabla_r [U(E_F)].$$

In the absence of spin broadening, Eq. (9) can be expressed as

$$n_0 = C_2 \sum_{n=0}^{n_{max}} [F_{1/2}(\eta_1) - F_{1/2}(\eta_2)] \tag{10}$$

where

$$C_2 = 2 \frac{B\sqrt{2m^*\pi}(k_B T)^{3/2}}{L_x h^2 E_0},$$

$F_j(\eta)$ is the one–parameter Fermi–Dirac integral of order j [21], $\eta_1 = (k_B T)^{-1}(E_F - E_2)$, $E_2 = [\left(n + \frac{1}{2}\right) \hbar\omega_0 - eE_0 L_x + (m^* E_0^2/2B^2)]$, $\eta_2 = (k_B T)^{-1}(E_F - E_3)$ and $E_3 = E_2 + eE_0 L_x$. Under the condition $E_0 \to 0$, Eq. (10) gets simplified to the well–known form [22]:

$$n_0 = N_C \Theta \sum_{n=0}^{n_{max}} F_{-1/2}(\eta) \tag{11}$$

where

$$N_C = 2 \left(\frac{2\pi m^* k_B T}{h^2} \right)^{3/2}, \quad \Theta = \frac{\hbar\omega_0}{k_B T}$$

and

$$\eta = \frac{1}{k_B T} \left[E_F - \left(n + \frac{1}{2}\right) \hbar\omega_0 \right].$$

3. Results and discussion

Using the appropriate equations together with the parameters $E_{01} = 0.05$ eV, $m^* = 0.067m_0$, $d_0 = 6$ nm, $T = 4.2$ K, $T_D = 9.3$ K, $g_0 = 2$ and $E_0 = 10^3$ V/m [23] for GaAs/AlAs SL, we have plotted the normalized $m_z^*(n, E_F)$ for the first two magnetic subbands as functions of n_0 and $1/B$ (Figs. 1 and 2, respectively). Using the same parameters as used in obtaining Figs. 1 and 2, we have further plotted $m_y^*(n, E_F)$ for the first two magnetic subbands as functions of n_0 and $1/B$ (Figs. 3 and 4, respectively), where we have also plotted $m_y^*(n, E_F)$ for GaAs for the purpose of comparison. From the above discussions and figures, the following features follow:

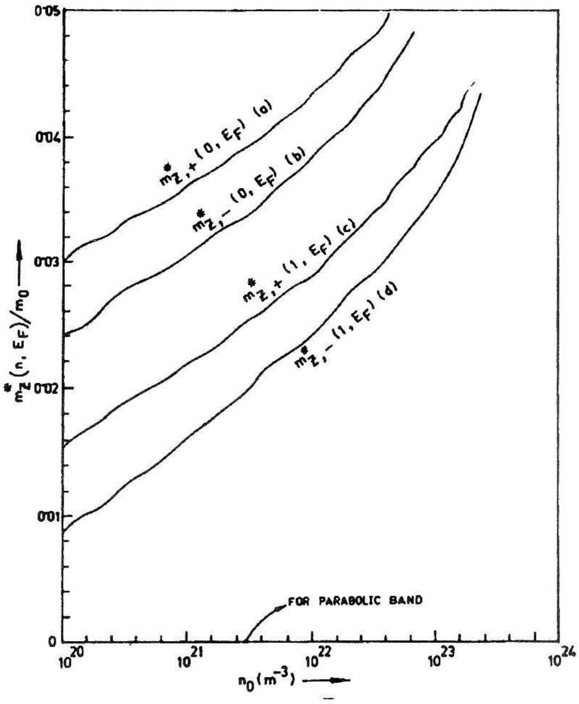

Fig. 1. Plot of the normalized $m_z^*(n, E_F)$ versus n_0 for the first two magnetic subbands in GaAs/AlAs SL under cross–field configuration ($B = 2$ T).

1. The band non–parabolicity in a non–parabolic material can alone explain the energy dependence of the effective electron mass along the direction of magnetic quantization but can not account for the dependence of the same mass on the magnetic quantum number at any given value of the electron energy [8]. It appears from Eq. (3) that the EMM along the z-direction in SL structure depends on the Fermi energy, Landau number and the spin splitting. This is a characteristic feature of the SL structure only and is independent of band non–parabolicity. The effective mass in the constituent bulk materials is a constant quantity along the z-

direction. It appears from Fig. 1 that $m_z^*(n, E_F)$ for the SL structure increases in an oscillatory way with increasing electron concentration and the index–dependent effective masses exhibit converging tendency for relatively higher values of the carrier degeneracy.

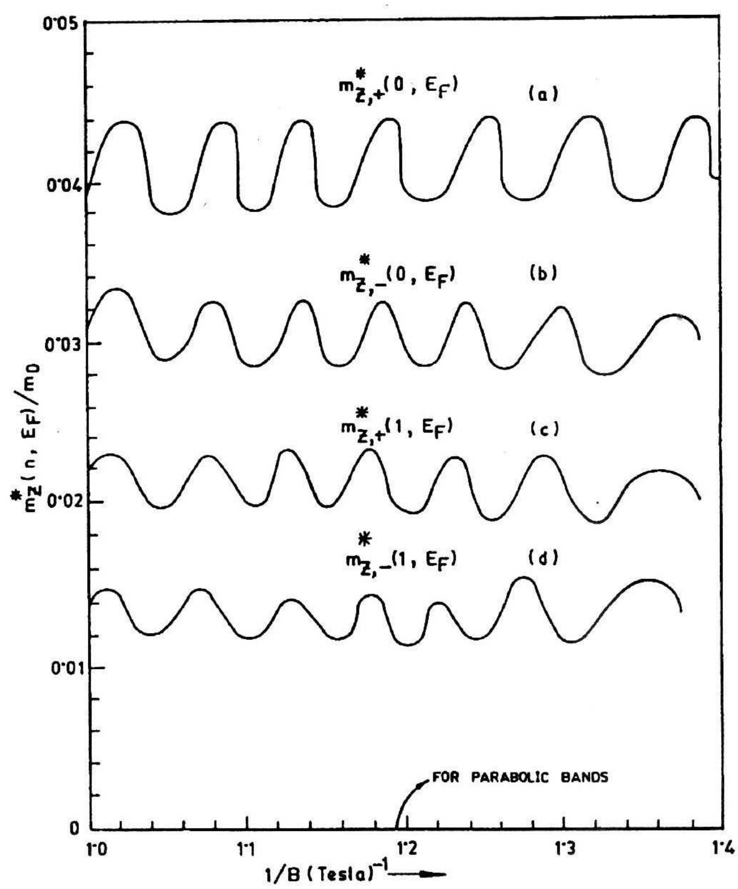

Fig. 2. Plot of the normalized $m_z^*(n, E_F)$ versus $1/B$ for the first two magnetic subbands in GaAs/AlAs *SL under cross–field configuration ($n_0 = 10^{23}$ m^{-3}).*

2. It appears from Fig. 2 that $m_z^*(n, E_F)$ oscillates with the reciprocal quantizing magnetic field. The oscillations are due to the Shubnikov–de Haas (SdH) effect. The SdH oscillations, which occur in degenerate materials, would further be influenced by the index dependent EMM in the present case and the contribution of the EMM on the oscillatory mobility would be important.

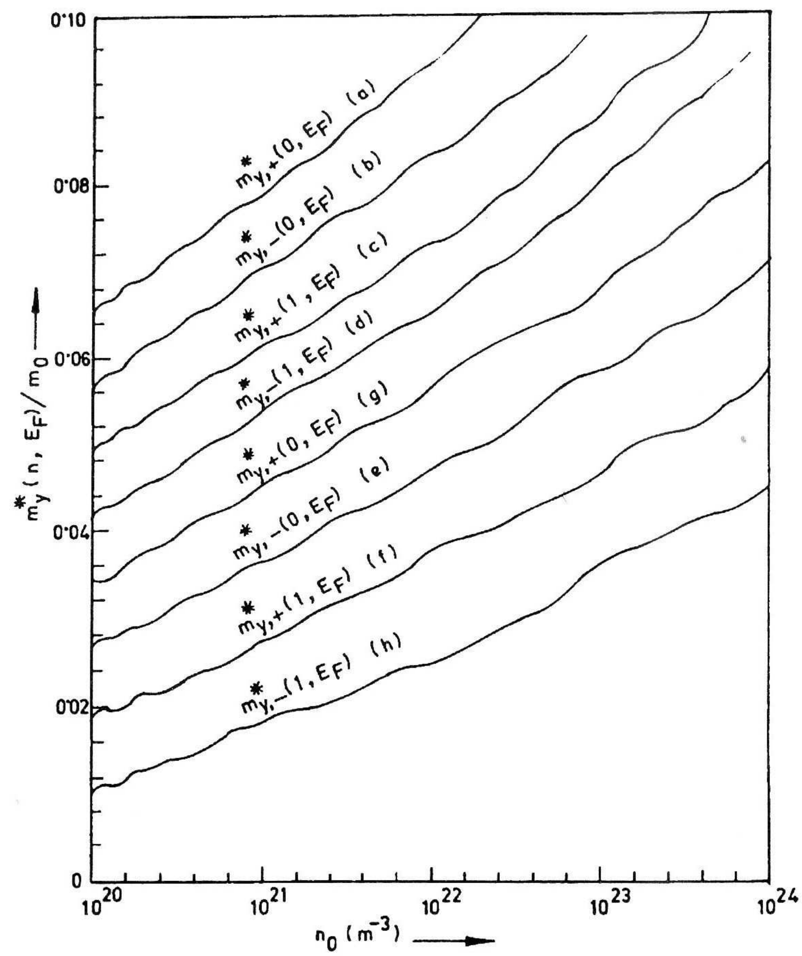

Fig. 3. Plot of the normalized $m^*_y(n, E_F)$ versus n_0 for the first two magnetic subbands in GaAs/AlAs *SL under cross–field configuration. The plots* e, f, g *and* h *exhibit the same dependence for GaAs ($B = 2$ T).*

3. The dependence of $m^*_y(n, E_F)$ on the magnetic quantum number and the Fermi energy is an inherent property of cross–fields. It appears from Eqs. (4) and (8) that under the condition $E_0 \to 0$, $m^*_y(n, E_F) \to \infty$ as it should. This statement is valid for both SL and the constituent materials under cross–field configuration. It appears from equations (7) and (8) that the cross–fields introduce the mass anisotropy which depends on the Fermi energy, spin–splitting and the Landau quantum number.

4. The electron concentration and the magnetic field influence $m^*_y(n, E_F)$ for both SL and the constituent materials under cross–field configurations, though the

nature of variations are different for different plots. The EMM's corresponding to $n = 0$ exhibits the greatest numerical values as appears from all the figures.

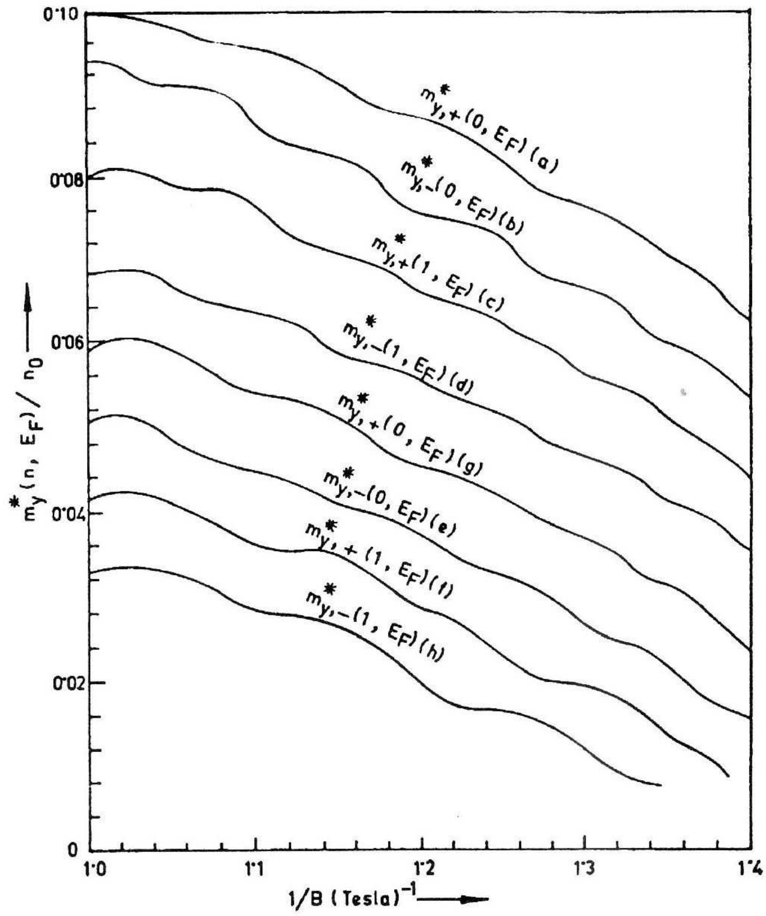

Fig. 4. Plot of the normalized $m^*_z(n, E_F)$ versus $1/B$ for the first two magnetic subbands in GaAs/AlAs *SL under cross–field configuration. The plots* e, f, g *and* h *exhibit the same dependence for GaAs ($n_0 = 10^{23}$ m^{-3}).*

Experimental data for comparison to our results are not available to the best of our knowledge. The expressions as given by Eqs. (3), (4), (5c), (8) and (9) are new and would be useful in analysing the experimental results when they appear. The variations of the EMM's are totally band structure dependent. With different sets of energy band constants, we shall get different numerical values of the EMM's, but the nature of variations will be unaltered. We have not plotted the EMM with other physical variables of considered other subbands for the purpose of condensed presentation. Finally, it may be noted that the basic aim of our present paper is not solely to demonstrate the effect of cross-field configuration on the EMM of the SL and the electron concentration in the respective cases since the formulations of the various transport coefficients depend on the electron statistics in such materials.

References

1) S. Adachi, J. Appl. Phys. **58** (1985) 11;
2) R. Dornhaus and G. Nimtz, Springer Tracts in Modern Physics **78** (1976) 1;
3) W. Zawadzki, *Handbook of Semiconductor Physics*, Amsterdam, North Holland, **1** (1982) 719;
4) I. M. Tsidilkovskii, *Band Structure of Semiconductors*, Pergamon Press, Oxford, 1982;
5) V. K. Arora and H. Jaafarian, Phys. Rev. **B13** (1976) 4457;
6) R. Rossler, Solid State Commun. **49** (1984) 943;
7) B. Mitra, A. Ghoshal and K. P. Ghatak, Nuovo Cimento **12D** (1990) 891;
8) A. N. Chakravarti, K. P. Ghatak, K. K. Ghosh, S. Ghosh and A. Dhar, Z. Physik B **47** (1982) 149;
9) K. P. Ghatak and S. N. Biswas, Proceedings of the Photo–Optical and Instrumentation Engineers (SPIE, USA) **1484** (1991) 149;
10) B. Mitra and K. P. Ghatak, Solid State Electronics **32** (1989) 177; M. Mondal and K. P. Ghatak, Proceedings of the Materials Research Society (MRS, USA) **EA-16** (1988) 173;
11) F. Capasso, Semiconductors and Semimetals **22** (1985) 1;
12) F. Capasso, K. Mohammed, A. Y. Cho, R. Hull and A. L. Hutchinson, Appl. Phys. Lett. **47** (1985) 420;
13) M. Heiblum, D. C. Thomas, C. M. Knoedler and M. I. Nathan, Appl. Phys. Lett. **47** (1985) 1105;
14) K. Ploog and G. H. Dohler, Adv. Phys. **33** (1983) 285;
15) B. A. Wilson, IEEE Trans. Quantum Electronics **24** (1988) 1783;
16) W. Zawadzki, Surface Science **37** (1973) 218;
17) W. Zawadzki and B. Lax, Phys. Rev. Lett. **16** (1966) 1001;
18) D. Mukherjee, A. N. Chakravarti and B. R. Nag, Phys. Stat. Sol. (a) **26** (1974) 27;
19) M. Mondal, S. Banik and K. P. Ghatak, Canadian J. Phys. **67** (1989) 72;
20) A. N. Chakravarti, K. P. Ghatak, A. Dhar, K. K. Ghosh and S. Ghosh, Applied Physics (Springer Verlag) **A26** (1981) 165;
21) K. P. Ghatak, B. De and M. Mondal, Phys. Stat. Sol. (b) **165** (1991) K53;
22) J. S. Blakemore, *Semiconductor Statistics*, Dover Publications, New York, 1987;
23) M. Newberger, *Electronic Materials*, Vol. 2, Plenum Press, New York, 1991.

UTJECAJ UKRIŽENOG ELEKTRIČNOG I MAGNETSKOG POLJA NA EFEKTIVNU ELEKTRONSKU MASU U POLUVODIČKIM SUPER–REŠETKAMA

KAMAKHYA P. GHATAK i SHAMBHU N. BANIK*

Department of Electronic Science, University of Calcutta, University College of Science and Technology, 92, Acharya Prafulla Chandra Road, Calcutta 700009, Indija
**Department of Physics, Dandirhat Nagendra Kumar Uchcha Siksha Niketan, P. O. Dandirhat, Dt. North 24 Parganas, West Bengal, Indija*

UDK 538.915

PACS 71.25.Jd

Proučavana je efektivna elektronska masa na Fermijevu nivou u poluvodičkim super–rešetkama u konfiguraciji ukriženih polja i uspoređena je s odgovarajućim veličinama sastavnih materijala, uzimajući kao primjer super–rešetku GaAs/AlAs. Ustanovljeno je da efektivna elektronska masa duž oba smjera ovisi također o magnetskom kvantnom broju. Karakterističan oblik ukriženih polja dovodi do oscilatorne anizotropije mase koja ovisi o indeksu gradbenih materijala. Numeričke vrijednosti mase u super–rešetkama su veće nego u pojedinim komponentama. Dobro poznati rezultati za slučaj odsustva električnog polja također su dobiveni iz našeg općenitog razmatranja u nekim graničnim uvjetima.